Supporting Information for "Gold(I) sulfide: unusual bonding and an unexpected computational challenge in a simple solid"

D. Santamaría-Pérez,* T. Marqueño, and R. Chulia-Jordan
Departamento de Física Aplicada-ICMUV, Universidad de Valencia,
MALTA Consolider Team, Edificio de Investigación,
C/Dr. Moliner 50, E-46100 Burjassot, Valencia, Spain.

D. Daisenberger
Diamond Light Source, Didcot OX11 0DE, Oxon, UK

J. Ruiz-Fuertes
DCITIMAC, Universidad de Cantabria, Avenida de Los Castros 48, 39005 Santander, Spain

C. Muehle and M. Jansen
Max-Planck-Institut für Festkörperforschung,
Heisenbergstrasse 1, 70569 Stuttgart, Germany

P. Rodriguez-Hernandez and A. Muñoz
Departamento de Física, Instituto de Materiales y Nanotecnología,
Universidad de La Laguna, MALTA Consolider Team, E-38206 La Laguna, Tenerife, Spain.

Erin R. Johnson
Department of Chemistry, Dalhousie University,
6274 Coburg Road, Halifax, Nova Scotia, Canada B3H 4R2

A. Otero-de-la-Roza
Departamento de Química Física y Analítica,
Facultad de Química, Universidad de Oviedo, 33006 Oviedo, Spain

(Dated: January 15, 2019)

I. CALCULATED BAND STRUCTURE

The following band structure was obtained using the PBE functional with the PAW/plane-waves approach at the equilibrium geometry. The rest of the calculation details are in the "Computational details" section of the main text.

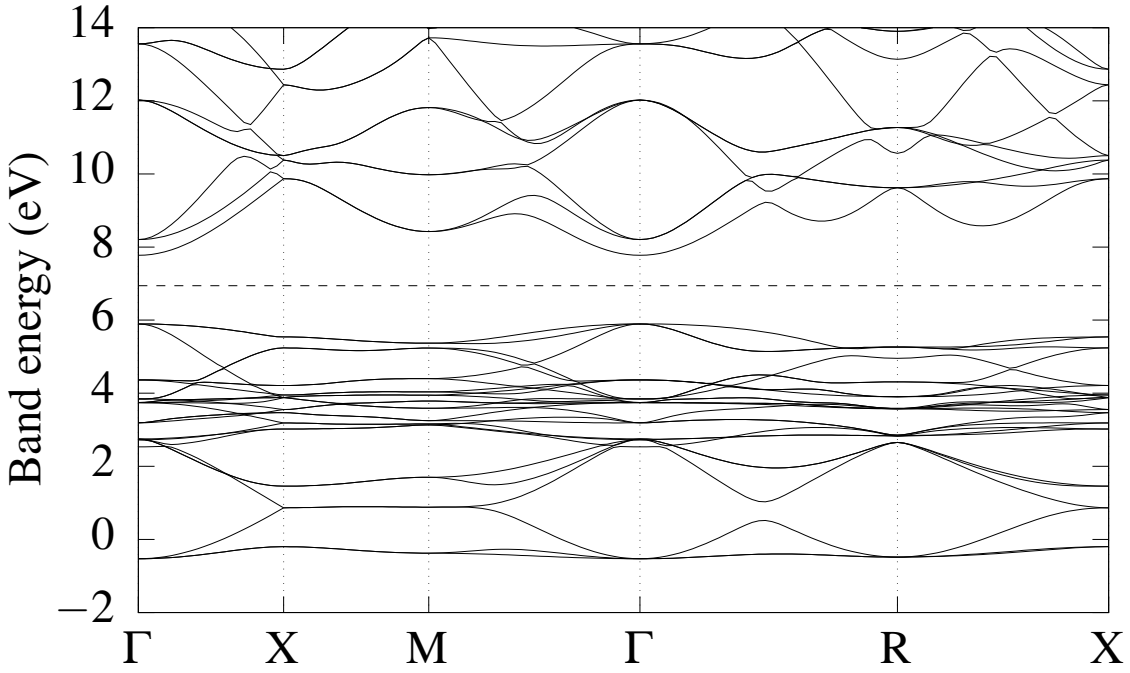

II. EXPERIMENTAL HIGH-PRESSURE BEHAVIOR OF GOLD SULFIDE

Figure 1 shows the region of interest of several X-ray diffraction (XRD) patterns at selected pressures and room temperature, where the pressure-induced amorphization (PIA) process can be easily observed. To quantify this phenomenon we compare the intensity of the Au_2S (111) peak to that of the Au (111) peak (Au is also present as an impurity in the Au_2S sample). Figure 2a shows the exponential decay of the $Au_2S(111)/Au(111)$ peak intensity ratio with increasing pressure, until the virtual disappearance of the gold sulfide reflections (Figure 1a). The logarithm of the intensity ratio as a function of pressure is shown in Figure 2b, illustrating the progressive amorphization of Au_2S with increasing pressure, and a step change between 26–28 GPa. As shown in the figure, the crystallinity of the Au_2S sample disappears at the same pace as the intensity of its strongest reflection:

$$\log(I_{\mathrm{Au_2S}}(111)/I_{\mathrm{Au}}(111)) = 0.947(9) - 0.0569(8)\Delta P \tag{1}$$

where P is the pressure in GPa. The non-linear behavior above 26 GPa is likely due to kinetic effects, since the sample was left at that pressure for a longer time prior to data collection. Parallel to the disappearance of the Bragg Au_2S peaks, a broad diffuse scattering band appears which is attributed to the amorphization of the sample.

Remarkably, the degree of crystallinity increases during decompression, as illustrated in Figure 1b. However, the return of crystallinity shows a hysteresis and the Au_2S sample is not com-

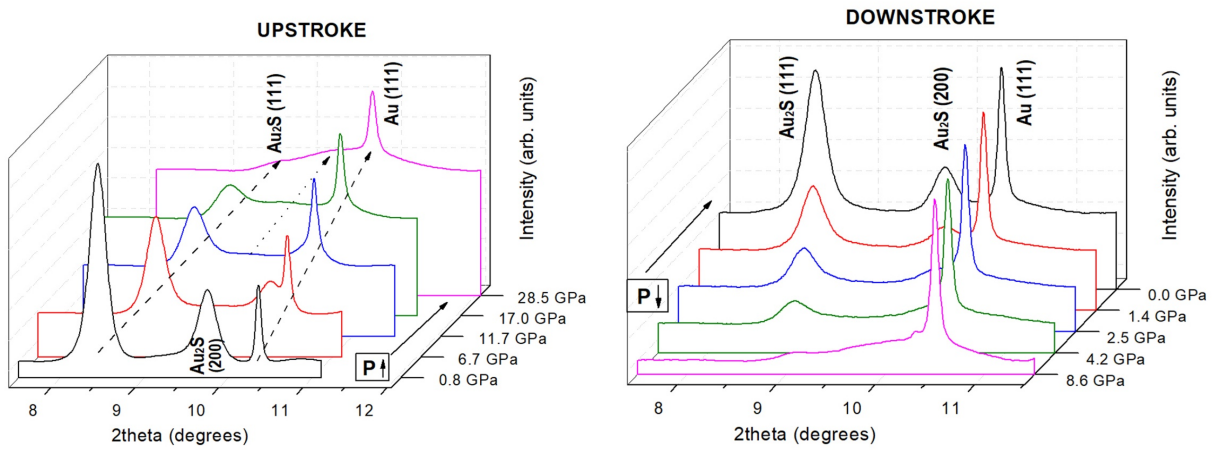

FIG. 1. XRD powder patterns of A_2S + Au impurity at selected pressures (a) upstroke to 29 GPa, the maximum pressure attained in our quasi-hydrostatic compression experiment using Ne as the pressure-transmitting medium, and (b) downstroke to ambient conditions. Backgrounds were subtracted. The gradual pressure-induced amorphization (PIA) process and the partial recovery of the degree of crystallinity during decompression can be observed.

pletely restored to its initial conditions. According to the aforementioned relative crystallinity gauge, only 30% of the initial Au_2S was recovered after compression (see Figure 2a). The rest could remain as amorphous material and/or could have decomposed into metallic gold and sulfur or a S-richer gold compound, although no evidences of these additional phases appear in the XRD patterns. The reversion back to the original structure after PIA has been observed in a number of compounds[1] and was interpreted as follows: The material amorphizes when it is compressed at temperatures that are sufficiently low to kinetically hinder an equilibrium phase transition. However, the atoms do not move far from their original positions, in such a way that on decompression they can go back to the thermodynamically stable ordered structure. The existence of some kinetic effects is consistent with (i) an observed 0.7% unit cell volume expansion and (ii) an observed 8% increase in the degree of crystallinity in the recovered Au_2S sample after allowing it to relax for 3 days.

Our data allows a restricted structural analysis under pressure. As mentioned, above 3.5 GPa only the (111) and (200) peaks of Au_2S can be discerned, and above 8 GPa only the (111) reflection is visible. Consequently, few categorical statements are possible. The XRD patterns show that initial $Pn\bar{3}m$ cubic Au_2S sample does not undergo any phase transition below 8 GPa. No additional peaks were observed and the possibility of a group-subgroup second-order phase transition (to rhombohedral, tetragonal or lower symmetry phases), with a distortion of the unit cell lattice

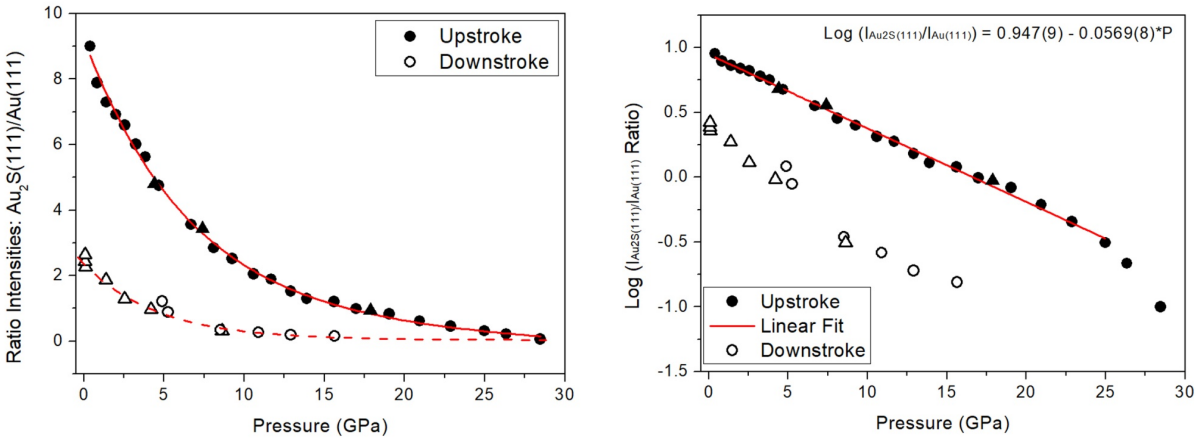

FIG. 2. (a) Intensity ratio and (b) logarithm of the intensity ratio of Au_2S and Au (111) peaks as a function of pressure. All data are from experiment with Ne as pressure medium. During compression Au_2S undergoes progressive amorphization. The degree of crystallinity is gradually restored during decompression, but this behavior shows hysteresis. Only 30% of the initial Au_2S was recovered after decompression.

parameters caused by the slight displacement atomic positions, was ruled out because it would entail the splitting of the (111) and (200) peaks. Thus, in this pressure range, the structure remains cubic with the Au and S atoms in special Wyckoff positions, meaning that the [Au4S] tetrahedra shrink but do not distort. Above 8 GPa, the data quality prevents any further analysis.

Regarding the compressibility of Au_2S, the lattice parameter of the cubic unit cell varies smoothly with increasing pressure, which also supports the absence of first-order phase transitions in the whole pressure range of this study. The absolute contraction of the unit cell axis between room pressure and 29 GPa is 0.704 Å, i.e. 14%. The least-squares fits of third-order Birch-Murnaghan (BM) EOS[2] to our experimental and theoretical unit-cell volume data are collected in Table I of the main text, and a detailed plot of the experimental fittings is shown in Figure 3. Gold sulfide has a low bulk modulus. This high compressibility is comparable to that of low-pressure phases of alkali metal binary sulfides[3–6] and slightly larger than that reported for the low pressure phases of other group 11 sulfides such as Cu_2S,[7,8], AgCuS[9] and Ag_2S.[10] Secondly, as illustrated in Figure 3, the experimental data cannot be properly fitted using a 3rd-order BM-EOS due to the existence of two different pressure regimes, below and above 8 GPa. The Au_2S structure is considerably more compressible at low pressures. This change in the compressibility behavior might be caused by a second-order phase transformation which would reduce the internal symmetry by alteration of the local atomic environments. Finally, as can be also seen from the data shown in Figure 5, there is a large hysteresis in the volume during decompression, the degree of which is also

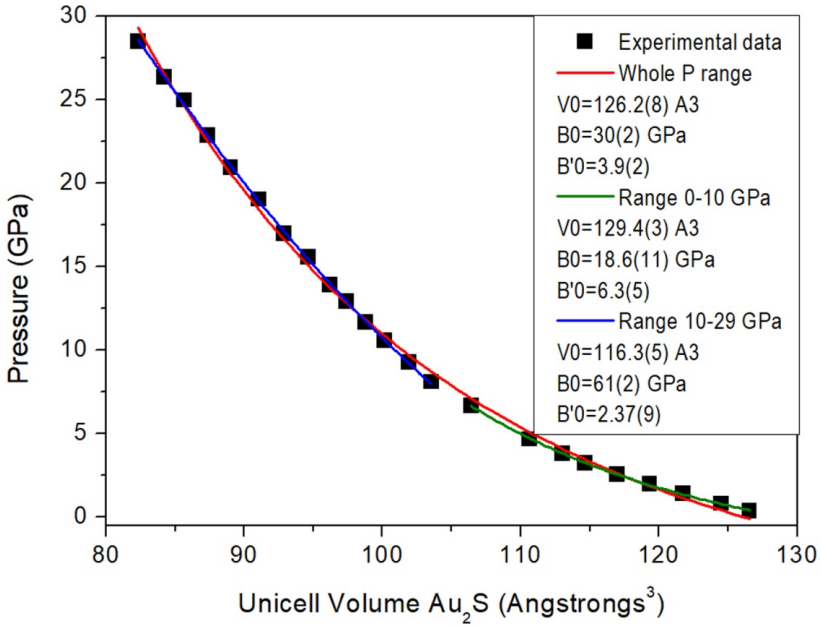

FIG. 3. Fits of the high-pressure room-temperature experimental data using Ne with a third-order Birch-Murnaghan EOS. The whole experimental dataset cannot be fitted properly due to a change of compressibility above 8 GPa. The Au_2S structure is considerably more compressible at low pressures.

dependent on the maximum pressure and/or the pressure transmitting media. This fact entails that the P-V data upon decompression describes a completely different curve which only can be fitted by a 3rd-order BM-EOS with a large first bulk modulus pressure derivative: $V_0 = 130(3)$ Å^3, $B_0 = 8(3)$ GPa, and $B_0' = 12(4)$.

---

* dsantamaria@quim.ucm.es

[1] Kruger, M.; Jeanloz, R. Memory glass: an amorphous material formed from AlPO4. *Science* **1990**, *249*, 647–649.

[2] Birch, F. Finite strain isotherm and velocities for single-crystal and polycrystalline NaCl at high pressures and 300 K. *J. Geophys. Res.* **1978**, *83*, 1257–1268.

[3] Grzechnik, A.; Vegas, A.; Syassen, K.; Loa, I.; Hanfland, M.; Jansen, M. Reversible antifluorite to anticotunnite phase transition in Li2S at high pressures. *J. Solid State Chem.* **2000**, *154*, 603–611.

[4] Vegas, A.; Grzechnik, A.; Syassen, K.; Loa, I.; Hanfland, M.; Jansen, M. Reversible phase transitions in Na2S under pressure: a comparison with the cation array in Na2SO4. *Acta Cryst. B* **2001**, *57*, 151–156.

[5] Vegas, A.; Grzechnik, A.; Hanfland, M.; Mühle, C.; Jansen, M. Antifluorite to Ni2In-type phase transition in K2S at high pressures. *Solid State Sci.* **2002**, *4*, 1077–1081.

[6] Santamaria-Perez, D.; Vegas, A.; Muehle, C.; Jansen, M. High-pressure experimental study on Rb2S:

antifluorite to Ni2In-type phase transitions. *Acta Cryst. B* **2011**, *67*, 109–115.

[7] Santamaria-Perez, D.; Garbarino, G.; Chulia-Jordan, R.; Dobrowolski, M.; Mühle, C.; Jansen, M. Pressure-induced phase transformations in mineral chalcocite, Cu2S, under hydrostatic conditions. *J. Alloys Compds.* **2014**, *610*, 645–650.

[8] Zimmer, D.; Ruiz-Fuertes, J.; Morgenroth, W.; Friedrich, A.; Bayarjargal, L.; Haussühl, E.; Santamaría-Pérez, D.; Frischkorn, S.; Milman, V.; Winkler, B. Pressure-induced changes of the structure and properties of monoclinic α-chalcocite Cu_2S. *Phys. Rev. B* **2018**, *97*, 134111.

[9] Santamaria-Perez, D.; Morales-Garcia, A.; Martinez-Garcia, D.; Garcia-Domene, B.; Muhle, C.; Jansen, M. Structural phase transitions on AgCuS stromeyerite mineral under compression. *Inorg. Chem.* **2012**, *52*, 355–361.

[10] Santamaría-Pérez, D.; Marqués, M.; Chuliá-Jordán, R.; Menendez, J. M.; Gomis, O.; Ruiz-Fuertes, J.; Sans, J. A.; Errandonea, D.; Recio, J. M. Compression of Silver Sulfide: X-ray Diffraction Measurements and Total-Energy Calculations. *Inorg. Chem.* **2012**, *51*, 5289–5298.